

## ORIGINAL ARTICLE

# Optimized low pH formulation of niacinamide enhances induction of autophagy marker ATG5 gene expression and protein levels in human epidermal keratinocytes

J.E. Oblong,\* Y.M. DeAngelis, B.B. Jarrold, J.C. Bierman, H.A. Rovito, L. Vires, B. Fang, T. Laughlin, W. Zhao, S.M. Hartman, R. Kainkaryam, R. Adams, J.D. Sherrill, T. Hakozaiki

The Procter & Gamble Company, Cincinnati, OH, USA

\*Correspondence: J.E. Oblong. E-mail: oblong.je@pg.com

## Abstract

**Background** Macromolecules in skin cells are damaged when exposed to environmental stressors, leading to disrupted cellular function and homeostasis. While epidermal turnover can eliminate some of this damage, autophagy can rapidly remove these defective components. Niacinamide (Nam) is known to induce autophagy and optimizing formulations to maximize this response could provide improved homeostasis in stressed skin.

**Objective** To determine (i) whether Nam can induce autophagy related 5 (ATG5), an autophagy marker, in human keratinocytes and (ii) whether optimized low pH Nam formulations can enhance the response in 3D skin models.

**Methods** Human keratinocytes treated with Nam were evaluated for autophagosome accumulation and induction of ATG5 by gene expression, immunoblotting and immunofluorescence microscopy. 3D skin equivalents were topically treated with Nam formulations at pH 5.8 and 3.8. Gene expression profiling and immunoblot analysis of ATG5 were performed.

**Results** Nam treatment of keratinocytes led to an accumulation of autophagosomes with a maximal signal at 48 h. Gene expression of ATG5 was induced by Nam, and immunoblots stained for ATG5 showed a significant increase after 6 h of treatment. Gene expression profiling of 3D epidermal skin equivalents treated with Nam at pH 3.8 showed stronger induction of autophagy-related genes, including ATG5, compared with pH 5.8 formulas. Enrichment for gene ontology terms on autophagy showed an increased linkage with Nam formulas at pH 3.8.

**Conclusions** We found that Nam induces autophagosome accumulation and ATG5 levels in keratinocytes. We also discovered that a Nam formulation at pH 3.8 can further increase levels of ATG5 in 3D skin models when compared to Nam at pH 5.8. These data support that Nam can induce autophagy in keratinocytes and formulations at pH 3.8 can enhance the impact. We hypothesize that optimized formulations at pH 3.8 can improve skin ageing appearance via autophagy induction.

Received: 8 March 2020; Revised: 16 April 2020; Accepted: 30 April 2020

## Conflict of interest

None.

## Funding sources

This work was funded by The Procter & Gamble Company.

## Introduction

Human skin is the largest organ and serves a critical role in protecting the body from damaging environmental stressors such as solar radiation, pollutants and microbial invasion. The epidermal compartment of skin is the first line of defence and facilitates removal of any sustained cellular damage via continuous renewal through a balanced programme of proliferation and differentiation that occurs over a 24- to 28-day period. However, stress exposure can cause immediate damage to macromolecules

(e.g. DNA, protein and lipids) that can lead to oxidative stress, inflammation and cellular dysfunction. Thus, it is necessary to rapidly and efficiently remove damaged macromolecules and thereby maintain cellular homeostasis to prevent premature ageing and maintain skin health.

Autophagy is an essential housekeeping cellular process, which is required to maintain homeostasis by monitoring and facilitating the removal of damaged intracellular components such as aggregated proteins and damaged organelles (e.g.

mitochondria, endoplasmic reticulum, nucleus and peroxisomes). Damaged materials are encircled into autophagosomes which then fuse with lysosomes to ultimately breakdown debris into recycled components or exported ones for removal from the cell. Under stress conditions, autophagy is essential in ensuring there is rapid removal of damaged components to prevent induction of apoptosis and senescence.<sup>1</sup> As in all organs, autophagy plays a significant role in skin biology to help maintain homeostasis and prevent disease conditions.<sup>2,3</sup> In the epidermis, autophagy has been shown to play a role in terminal differentiation as measured by elevated activity in the granular layer.<sup>4</sup> Maintenance of efficient autophagy is hypothesized to also prevent premature skin ageing, particularly in photoexposed body sites.<sup>5</sup> Thus, a better understanding of autophagy in skin biology would allow for the identification of technologies that could maintain and enhance autophagy activity during stress and, ultimately, prevent ageing and maintain skin health.

Niacinamide (Nam; aka nicotinamide, vitamin B<sub>3</sub>) has been used for decades in cosmetic and pharmaceutical products for the treatment of acne, photoageing attributes and barrier integrity improvement.<sup>6–8</sup> It has been reported that Nam can protect cells from oxidative stress, UV-induced immunosuppression and metabolic disruption.<sup>9–11</sup> Mechanistically, it has become apparent that Nam can have a significant impact on numerous processes associated with skin homeostasis and ageing.<sup>12,13</sup> While the impact of Nam on autophagy has been less studied in skin cells, it has been reported that Nam can induce mitophagy, a select form of autophagy, in dermal fibroblasts.<sup>14</sup> Mechanistically it is believed that this is via increased NAD<sup>+</sup> cellular pools.<sup>15</sup> However, there have been no reports to date on the role of Nam on autophagy in epidermal keratinocytes.

Topical formulations containing Nam have historically been practiced within a neutral pH range to prevent formation of niacin, a known vasodilator. It is also known that acidic formulations at pH 4.0 can promote skin barrier function,<sup>16,17</sup> particularly in elderly skin where skin surface pH is more alkaline.<sup>18</sup> Interestingly, while it has been reported that acidic conditions *in vitro* can induce autophagy,<sup>19</sup> it is not known whether a topical formulation would have any impact on autophagy.

Based on this background context, we wished to understand what impact Nam could have on autophagy in cultured epidermal keratinocytes. Additionally, whether a topical application of Nam in a lower pH formulation would further enhance autophagy induction in 3D skin models. To determine this, we measured the impact of Nam on ATG5, a canonical marker of autophagy, in these skin models.

## Methods

### Cells and reagents

Telomerase-transfected keratinocytes (hTERT) were expanded in a CO<sub>2</sub>, 37°C incubator using Epilife™ (Thermo Fisher

Scientific, Waltham, MA, USA) media with human keratinocyte growth supplement and gentamicin/amphotericin B. Cells never exceeded 70% confluency nor passage 5. Human HaCaT keratinocytes were purchased from AddexBio (San Diego, CA, USA). Cells were grown in Epilife medium with 60 μmol/L calcium (Thermo Fisher Scientific) and supplemented with human Keratinocyte Growth Supplement (Thermo Fisher) and gentamicin/amphotericin B 500× solution (Thermo Fisher) in T-75 flasks (Corning, Oneonta, NY, USA). Cells were cultured at 37°C, 5% CO<sub>2</sub> and 90% relative humidity.

For ATG5 gene expression experiments, HaCaT keratinocytes were cultured and maintained in the same medium used for primary keratinocytes. The day before treatment, keratinocytes were plated in 12-well BIOCOAT plates, 100 000 cells/well in 2 mL media/well. The plates were incubated at room temperature 30–60 min to allow cells to attach evenly in wells and then moved to incubator (5% CO<sub>2</sub>, 37°C). On treatment day, the media removed before treatments added. At harvest, the media was removed and 350 μL RLT Buffer (Qiagen, Germantown, MD, USA) was added to each well before transferring lysates to tubes.

A 3D human epidermal skin organotypic model (EpiDerm™, MatTek Corporation, Ashland, MA, USA) was used to assay the effects of Nam. Briefly, epidermal cultures were received and allowed to acclimate overnight in Dulbecco's Modified Eagle's Medium with epidermal growth factor, insulin, hydrocortisone and proprietary stimulators of epidermal differentiation supplement and gentamicin/amphotericin B. An oil-in-water emulsion system was formulated at varying final pH values and with or without 2% Nam (final weight per volume). After treatment with the formulations, cultures were removed from media and sliced in half, flash frozen in liquid nitrogen and transferred to –80°C freezer.

### Cyto-ID® staining

Treated hTERT keratinocytes were stained using the Cyto-ID® Kit (Enzo Life Sciences, Farmingdale, NY, USA) per manufacturer instructions. The fluorescent readouts (excitation/emission 480/530 and 340/480 nm) were taken using a Synergy Neo plate reader (BioTek, Winooski, VT, USA). The ratios of the 480/530 readout over the 340/480 readouts were calculated for each sample, and the no treatment controls were used as the normalization denominator. Autophagosome upregulation was indicated when the ratio to control was statistically significantly higher than 1.00. Student's *t*-test, pairwise and equal variance, was used for statistical calculations.

### Immunoblot analysis

HaCaT keratinocytes were seeded in six-well tissue culture plates at 1.5 × 10<sup>5</sup> cells per well. Cells were treated with 1 mmol/L Nam (Sigma-Aldrich, St. Louis, MO, USA) for indicated times. For protein extraction, RIPA or T-Per buffer at time of use was

supplemented with Halt (Invitrogen, Carlsbad, CA, USA) protease inhibitor tablet and phosphatase inhibitor cocktails 100×; 10 µL/mL (T-Per + PPI). Cells cultured in six-well plates were lysed and collected in RIPA + PPI buffer (Invitrogen). Cells were sonicated on ice in a sonicating water bath for 30 min. Lysate was centrifuged at 18 000 × g for 15 min at 4 °C. After centrifugation, the supernatant was collected in a fresh Eppendorf tube. MatTek Epidermis 3D cultures were removed from freezer, the collagen membrane removed and discarded, and 300 µL of T-Per + PPI was added to each sample, along with a 5 mm stainless steel bead (Qiagen). The samples were bead-beated using a Qiagen Tissue Lyser for 30 s at the 30 mHz. The samples were placed in a Branson sonicating water bath and sonicated on ice for 30 min. Lysate was centrifuged at 18 000 × g for 15 min at 4 °C. After centrifugation, the supernatant was collected in a fresh Eppendorf tube and was labelled.

Protein concentration was obtained using a BCA assay (Pierce, Waltham, MA, USA). Same amount of protein mixed with 4× Bolt LDS Sample buffer and 10× Bolt Sample reducing Agent (Invitrogen). The samples were heated to 100 °C for minimum of 5 min and loaded onto a Bolt™ 12% Bis-Tris Plus Gels, 12-well (Invitrogen) and ran at 200 V. A standard molecular weight ladder was loaded along with the samples to keep a track of the movement of the proteins in the gel. Proteins were transferred onto activated PVDF at 20 V for 120 min and left overnight. The membrane was removed on completion of the transfer and dried for 60 min. Membranes were wetted with methanol followed by thorough rinsing of the membrane with deionized water. After blocking with 5% blocker, BSA in 1× PBS/Tw (20× PBS Tween 20) for 60 min at room temperature, washed 3× with PBS/Tw, the membrane was incubated with specific primary antibodies (1 : 2000 dilution) in 1% blocker, BSA in PBS/Tw for 60 min at room temperature. The membranes were then washed three times with PBS/Tw before the addition of secondary antibody. The secondary antibody, also prepared in 1% blocker, BSA, was incubated with the membrane for 60 min at room temperature. The dilution of the secondary antibody was generally kept at 1 : 10 000 for goat anti-rabbit IgG (H + L) secondary antibody, HRP. The membranes were then washed again with PBST multiple times and developed using a mixture of equal volumes of developing solutions 1 and 2 for ECL or imaged directly for fluorescence signal detection using LICOR Image Studio software (LICOR, Lincoln, NE, USA). Densitometry was analysed using LICOR's Image Studio Digits software. Blots were stripped using LiCor Western Sure ECL Stripping buffer following LiCor's protocol. Then, re-blocked and probed with Anti-beta Actin antibody (mAbcam 8226) – Loading Control (HRP).

### Microarray analysis

Samples ( $n = 6$  per treatment group) were collected in RNALater buffer, flash frozen and stored at  $-80^{\circ}\text{C}$  prior to RNA extraction. RNA was extracted and purified using the RNeasy kit (QIAGEN).

Purified RNA was converted to biotin-labelled complementary RNA copies using the HT 3' IVT Express kit (Affymetrix, Santa Clara, CA, USA) per the manufacturer's protocol. Samples were then subjected to microarray profiling using GeneTitan U219 microarray plates (Affymetrix). Probe set expression values were calculated by quartile normalization and PLIER summarization algorithms. Principal component analysis and leave-one-out and leave-two-out prediction intervals identified no sample outliers. Test statistics comparing each treatment group to untreated cells at 24 h (NT24) was moderated using the empirical Bayes method from the limma R-package, and false discovery rates (FDR) were controlled using the Benjamini-Hochberg correction. A minimum expression threshold (>20th percentile in  $\geq 50\%$  of replicate samples within a treatment group) was set to filter out low-expressed probe sets using GeneSpring v14.9.1 (Agilent Technologies, Inc., Santa Clara, CA, USA), and hierarchical clustering of autophagy gene probe sets by normalized intensity values was performed using the Euclidean distance and Ward's linkage method.

### Pathway analysis

Gene set enrichment analysis (GSEA) v4.0.3 was performed as previously described.<sup>20,21</sup> Random gene set permutation ( $n = 10\ 000$ ) was used to query the data against Gene Ontology<sup>22,23</sup> gene set annotations curated within MSigDB v7.0 database within the GSEA software.

### Transcriptional pattern matching to autophagy-inducing chemistries

A signature-free pattern matching algorithm based on Connectivity Mapping (CMap).<sup>24</sup> was developed and performed as similarly described.<sup>25</sup> In brief, the transcriptional profiles (i.e.  $\log_2$  fold change between a treatment group and untreated cells at 24 h) described herein were assessed for similarity (or dissimilarity) to the transcriptional profiles within the CMap database, which consists of >4200 chemistries (vs. DMSO control) in hTERT keratinocyte cell lines treated for 6 h. Fisher's discriminant analysis (FDA) was used to minimize batch-based variability and reduce the dimensionality of the data. To reduce over-fitting, a relaxed version of FDA was implemented in the R statistical programming language and applied to the CMap database. The signature-free pattern matching algorithm uses  $\sim 50\%$  of the measured probe sets ( $n = \sim 20\ 000$ ) to create a reduced-dimensional representation of the original expression profile data set of the various chemical treatments and ensures that two or more chemical replicates tested in different experimental batches show similar expression patterns. Transcriptional similarity is then assessed by calculating cosine distances (i.e. linkage scores), with linkage scores ranging from  $-1$  (more dissimilar) to  $1$  (more similar).

### Immunofluorescent staining

Immunofluorescent detection of the autophagy marker ATG5 was conducted in HaCaT keratinocytes cultured at  $37^{\circ}\text{C}$ ,  $20\% \text{O}_2$ ,

5% CO<sub>2</sub> and 90% relative humidity for 72 h prior to trypsinization. HaCaT keratinocytes were trypsinized from T-75 flasks incubated at 20% O<sub>2</sub> and plated at  $1 \times 10^4$  per well into  $\mu$ -slides (Ibidi 8 well) in 300  $\mu$ L of medium per well. Cells were treated with 1 mmol/L Nam (Sigma-Aldrich) for 6, 24, 48 and 72 h with media and treatment refreshed daily. Slides were incubated at 20% O<sub>2</sub> for length of treatment. Following incubation, cells were washed in PBS and fixed with ice cold methanol, permeabilized in 0.1% Triton X-100 in PBS and blocked for 1 h with 3% BSA in PBS. Cells were incubated overnight at 4°C with primary antibodies for ATG5 (Abcam 108327, 1 : 100, Cambridge, MA, USA), diluted in PBS containing an Alexa Fluor 488 conjugated Alpha Tubulin antibody (Abcam 195887, 1 : 250). Cells were washed in PBS and stained with Alexa Fluor 555 secondary antibodies (Abcam 150086, 1 : 1000) in PBS for 1 h at room temperature, washed and DAPI counter stained using NucBlue fixed cell stain ReadyProbes reagent (Invitrogen). Fluorescent images were captured with a Zeiss Z1 microscope (White Plains, NY, USA).

## Results

### Induction of autophagic flux by Nam over time in human epidermal keratinocytes

To understand the impact of Nam on autophagic flux in keratinocytes, we cultured hTERT keratinocytes under normal growth conditions and exposed to 400  $\mu$ mol/L Nam for 24 h. Image capture showed an increase in fluorescent puncta with Nam treatment compared with control cultures (Fig. 1a). Quantification of FITC signal normalized to DAPI staining showed a 36% increase in signal in Nam-treated cells over control (Fig. 1b). A time course experiment was performed to evaluate what impact Nam has on autophagic flux over time. hTERT keratinocytes were incubated with 400  $\mu$ mol/L Nam for up to 72 h and Nam treatment showed a significant increase in signal at all time points with a maximal 22% increase in signal at 72 h compared with control cells (Fig. 1c,  $P = 0.042$ ).

### Nam stimulates expression of the autophagy marker ATG5

To evaluate the impact of Nam on ATG gene expression and protein levels, HaCaT keratinocytes were exposed to 250  $\mu$ mol/L Nam for 6 h and then processed for microarray profiling. Nam increased expression of ATG5 by 1.05X fold change compared with vehicle control (Fig. 2a). To quantitate the changes in ATG5 due to Nam exposure, we performed immunoblot analysis of cell lysates (Fig. 2b) and quantitation showed a 19% increase in ATG5 protein levels after 6 h of treatment compared with the 99% increase by the positive control chloroquine (Fig. 2c, CQ). Interestingly, there was a steady increase in ATG5 levels but were not statistically significant compared with control treatments. Keratinocytes were stained for ATG5 and immunofluorescence photomicrographs showed an increase signal intensity with Nam treatment at 6 h (Fig. 2d). Quantitation of signal intensity

showed a 34% increase with Nam treatment compared with non-treated control cells at 6 h (Fig. 2e,  $P < 0.0001$ ). While the ATG5 signal levels were still significantly higher at 24 and 48 h, there was a steady decrease to baseline levels at 72 h.

### Topical application of Nam in 3D skin equivalent models shows an increase in ATG5 expression when formulated at pH 3.8 vs. 5.8

Acidic pH is known to promote skin barrier function as well as stimulate the molecular events leading to autophagy. Based on the 2D keratinocyte data, we hypothesized there was a combinatorial effect of Nam and low pH on autophagy-related gene transcription. To this end, microarray profiling was performed on 3D epidermal cultures treated topically with oil-in-water emulsion formulations containing Nam at pH 3.8 and 5.8. Nam at pH 3.8 induced a robust genome-wide changes in expression in a pH-dependent manner, with a maximum number of significantly regulated probe sets by Nam (3.8) treatment compared with untreated cells (Table 1). Vehicle at pH 2.5 or 5.8, however, induced only modest numbers of differentially regulated probe sets above random chance when compared to untreated cells. Notably, hierarchical clustering of genes involved in autophagy showed a strikingly similar expression pattern induced by Nam (5.8) and Nam (3.8) and that was distinct from untreated (NT24) and Veh (2.5) and (5.8)-treated cells (Fig. 3a). Indeed, several genes involved in autophagy initiation and autophagosome formation (beclin-1, *BECN1*; WD repeat domain, phosphoinositide interacting 2, *WIPI2*; SH3 domain containing GRB2 like, endophilin B1, *SH3GLB1*; and TBC1 domain family member 5, *TBC1D5*), autophagosome membrane elongation (autophagy related 5, *ATG5*), and substrate capture (NBR1 autophagy cargo receptor, *NBR1*) were significantly upregulated by low pH Nam treatments compared with untreated and low pH (2.5 and 5.8) alone (Fig. 3b).

We next sought to understand whether the global transcriptional changes induced by low pH Nam were associated with autophagy-related biological pathways using GSEA and Gene Ontology (GO) gene sets. Low pH Nam treatments were enriched for several GO pathways involved in autophagic processes, including *regulation of autophagosome assembly* (FDR  $q$ -values  $< 0.25$ ; Table 2). Moreover, several biological processes such as *regulation of vacuole organization*, *intrinsic component of peroxisomal membrane*, *peroxisome transport* and *organization and protein targeting to lysosome* associated with low pH Nam showed a pH-dependent enrichment as indicated by increasing normalized enrichment scores (NES) and/or decreasing FDR  $q$ -values from Nam (5.8) to Nam (3.8).

Pattern matching algorithms have proven useful for predicting similar (or dissimilar) mechanisms-of-action among unrelated pharmacological agents and/or diseased states based on differential gene expression.<sup>24</sup> Indeed, transcriptional similarities among several dermatological conditions and their reversal by

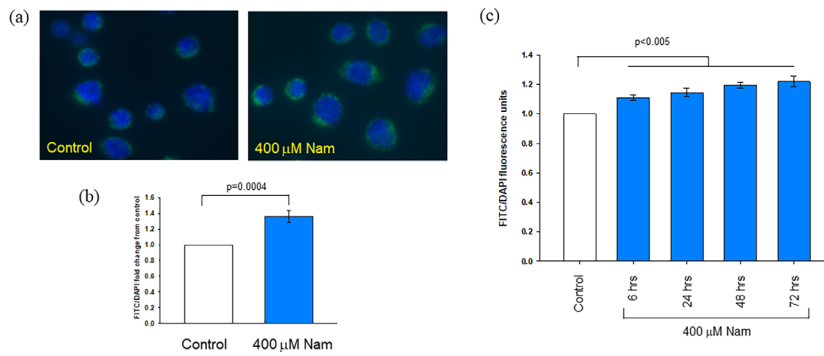


**Figure 1** Nam increases autophagic flux in keratinocytes. (a) Representative microscopic images of autophagic flux in hTERT keratinocytes treated with or without 400 μmol/L Nam for 24 h and stained with Cyto-ID<sup>®</sup> autophagy probe show elevated presence of green puncta in Nam treated cells. (b) Autophagic flux index was calculated by counting green puncta divided by the number of cells (DAPI-stained blue nuclei) in multiple fields. Nam treatment showed a 36% increase in fold change of flux index compared with control ( $P = 0.0004$ ). (c) hTERT keratinocytes were incubated with or without 400 μmol/L Nam up to 72 h. Autophagic flux calculations showed a 22% increase signal in cells incubated with Nam at 72 h compared with control ( $P = 0.042$ ). Student's *t*-test was used to calculate *P* values in reference to control cells ( $n = 16$ ). Nam, niacinamide.

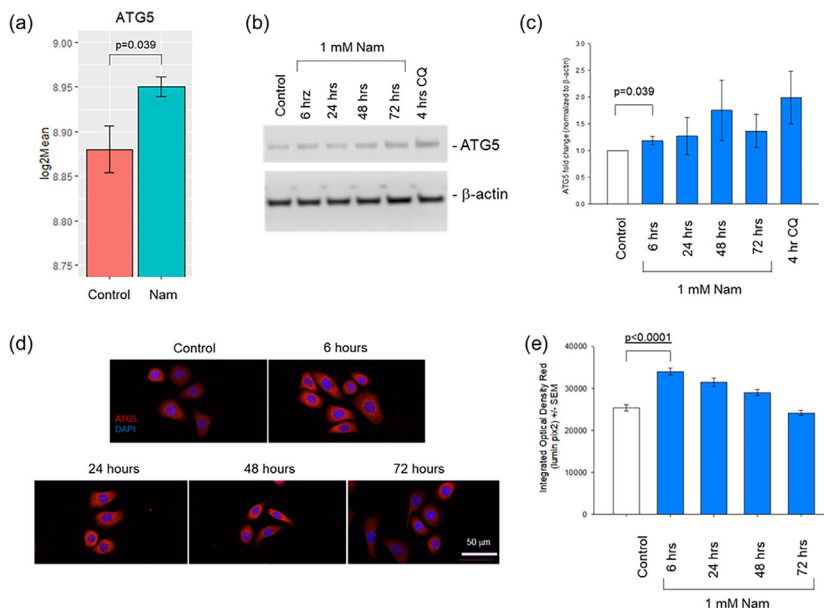


**Figure 2** Nam increases ATG5 gene expression and protein levels in keratinocytes. (a) Transcriptomics profiling comparing HaCaT keratinocytes treated with or without 250 μmol/L Nam for 6 h showed a 1.05× fold increase in ATG5 gene expression (Anova model,  $P = 0.0386$ ). (b) Immunoblot analysis for ATG5 from hTERT keratinocytes treated with 1 mmol/L Nam over 72 h. Control cells were treated with chloroquine (CQ) for 4 h to confirm signal induction. Cell extracts were prepared and analysed by immunoblotting using the indicated antibodies. β-Actin served as a control. (c) Densitometric analysis of the signals on the blots show a significant increase in ATG5 protein levels after 6 h of Nam treatment ( $P = 0.039$ ). (d) Immunofluorescence photomicrographs of HaCaT keratinocytes after treatment with 1 mmol/L Nam over 72 h. Select area from control and Nam treated cells at higher magnification (right panel). (e) Fluorescent signal intensity was quantitated ( $n > 190$  cells per treatment group) via image analysis and showed a 34% increase with Nam treatment compared with control cells at 6 h ( $P < 0.0001$ ). Nam, niacinamide.

known dermatological treatments as well as novel potential therapies has been demonstrated using pattern matching.<sup>25</sup> As several pharmacological agents have been shown to induce

autophagy (e.g. mTOR inhibitors),<sup>26</sup> we performed pattern matching on the low pH Nam treatments compared with untreated cultures and assessed similarities (positive linkage

**Table 1** Number of differentially expressed probe sets

Treatment	Probe sets (vs. untreated cells)	
	$P < 0.05$	$Q < 0.05$
Veh (pH 2.5)	2729	3
Veh (pH 5.8)	2947	8
2% Niacinamide (pH 5.8)	4875	590
2% Niacinamide (pH 3.8)	6201	1173

scores) to gene expression signatures generated from 2D keratinocytes treated with various autophagy-inducing agents. We observed positive linkages among the low pH Nam treatments with several autophagy-inducing agents (Table 3). In particular, mTOR-dependent autophagy inducers such as metformin, ridafolimus, temsirolimus, and torin-1 and -2, which showed positive linkages that increased from Nam (5.8) to Nam (3.8). These data suggest that low pH Nam may induce autophagy through an mTOR inhibitory mechanism.

### ATG5 immunoblot analysis of 3D skin models

After the finding that Nam formulated at pH 3.8 increased expression in autophagy-related gene ontology terms along with an increase in *ATG5* gene expression, we performed immunoblot analysis to quantify ATG5 protein levels. Total protein was

extracted from replicate 3D MatTek cultures treated with vehicle controls at pH 2.5 or pH 5.8 and 2% Nam at pH 5.8 and 3.8, separated on SDS-PAGE gels and transferred to PVDF. Immunoblot staining for ATG5 and  $\beta$ -actin (control) was performed (Fig. 4a). Densitometry quantitation showed that 2% Nam (pH 3.8) increased ATG5 signal intensity by 93% and 49% compared with pH 2.5 and 5.8 vehicle control, respectively, and a 49% increase compared with 2% Nam (pH 5.8; Fig. 4b).

### Discussion

Human skin's ability to protect the body from environmental insults requires efficient repair mechanisms so that stress induced damage is efficiently repaired or removed. The epidermis of skin undergoes a constant turnover process that facilitates the removal of damaged macromolecules, dysfunction organelles and pre-senescent cells. However, the turnover rate of the epidermis averages on the order of 28 days and it is critical for a more immediate intracellular repair response to prevent premature ageing, senescence onset and risk of pre-cancerous cellular transformation. Autophagy is a housekeeping cellular process that facilitates the recycling and removal of damaged macromolecule components such as proteins, lipids, DNA and organelles (reference). Under stress conditions, it's activity will dictate a cell's fate between repair to maintain viability and apoptosis.<sup>1</sup> Relative to skin, autophagy plays a significant role in

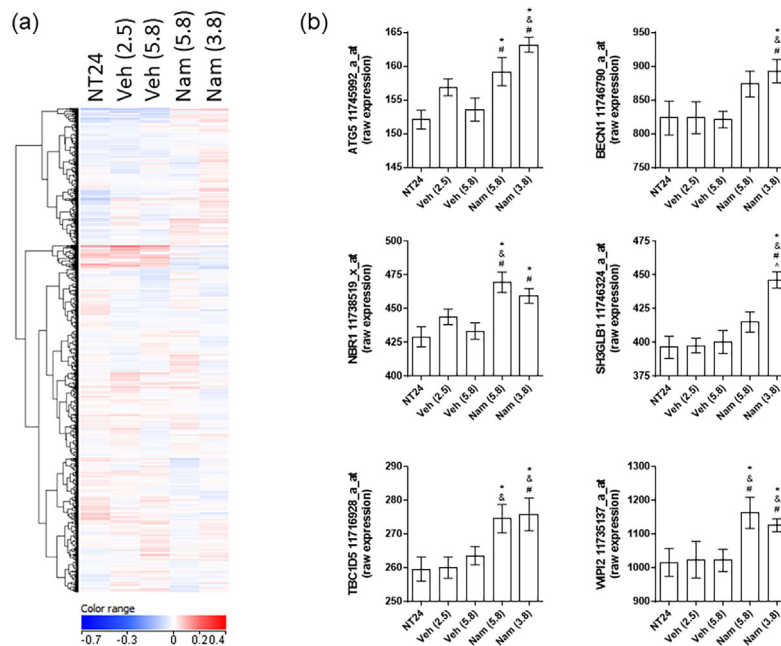


**Figure 3** Hierarchical clustering of autophagy-related gene expression. (a) Clustering of genes across untreated cultures (NT24) or cultures treated with vehicle at pH 2.5 (Veh 2.5), pH 5.8 (Veh 5.8), 2% Nam at pH 5.8 (Nam 5.8) or 2% Nam at pH 3.8 (Nam 3.8) harvested at 24 h. Colour range reflects normalized intensity values. (b) Raw expression profiles across conditions for probe sets of select autophagy genes. \* $P < 0.05$  vs. NT24;  $^{\&}P < 0.05$  vs. Veh (2.5);  $^{\#}P < 0.05$  vs. Veh (5.8);  $^{\wedge}P < 0.05$  vs. Nam (5.8). Nam, niacinamide.

**Table 2** Gene Set Enrichment of autophagy-related Gene Ontology terms across low pH niacinamide (Nam) treatments

GO term	Veh 2.5		Veh 5.8		Nam 5.8		Nam 3.8		
	NES	FDR q-val	NES	FDR q-val	NES	FDR q-val	NES	FDR q-val	
<b>Vacuole</b>	ESTABLISHMENT_OF_PROTEIN_LOCALIZATION_TO_VACUOLE		0.86	1	0.86	0.88	1.12	0.47	
	LATE_ENDOSOME_TO_VACUOLE_TRANSPORT	0.73	0.96	1.25	0.68	0.83	0.9	1.28	0.27
	LYTIC_VACUOLE_ORGANIZATION			0.81	1	1.19	0.47	1.41	0.17
	PROTEIN_CATABOLIC_PROCESS_IN_THE_VACUOLE	0.82	0.89	1.06	0.85	0.87	0.88		
	PROTEIN_LOCALIZATION_TO_VACUOLE			0.96	0.94	0.91	0.84	1.25	0.3
	PROTEIN_TARGETING_TO_VACUOLE					0.98	0.74	0.99	0.67
	REGULATION_OF_VACUOLE_ORGANIZATION	0.83	0.88			1.52	0.19	1.51	0.11
VACUOLE_ORGANIZATION					1.27	0.39	1.37	0.2	
<b>Peroxisome</b>	INTRINSIC_COMPONENT_OF_PEROXISOMAL_MEMBRANE		0.7	1	0.91	0.84	1.42	0.16	
	PEROXISOMAL_MEMBRANE_TRANSPORT	0.76	0.94	0.98	0.92			1.26	0.29
	PEROXISOMAL_TRANSPORT	0.91	0.80	1.29	0.61	1.46	0.23	1.92	0.01
	PEROXISOME_ORGANIZATION	1.04	0.63	1.44	0.48	1.61	0.15	2.06	0
	PEROXISOME_PROLIFERATOR_ACTIVATED_RECEPTOR_SIGNALING_PATHWAY			1.13	0.79				
<b>Lysosome</b>	ENDOLYSOSOME	1.81	0.07	0.93	0.96	1.03	0.67		
	ENDOSOME_TO_LYSOSOME_TRANSPORT	0.89	0.82	0.94	0.96				
	LYSOSOMAL_LUMEN	1.13	0.50	1.11	0.8	0.99	0.72	0.94	0.75
	LYSOSOMAL_TRANSPORT			0.97	0.93	1	0.7	1.16	0.41
	PROTEIN_LOCALIZATION_TO_LYSOSOME	0.94	0.76	1.11	0.8	0.83	0.91	1.24	0.31
	PROTEIN_TARGETING_TO_LYSOSOME	1.19	0.45	1	0.91	1.04	0.64	1.41	0.17
<b>Autophagy</b>	AUTOPHAGOSOME	1.18	0.46	0.89	0.99	1.38	0.28	1.09	0.51
	AUTOPHAGOSOME_MATURATION	1.18	0.46	1.08	0.84	1.36	0.29		
	AUTOPHAGOSOME_MEMBRANE	1.01	0.67	0.99	0.92	1.42	0.25	0.91	0.8
	AUTOPHAGOSOME_ORGANIZATION					1.36	0.29	1.21	0.35
	AUTOPHAGY_OF_MITOCHONDRION			1.08	0.84	1.5	0.2	1.18	0.39
	CHAPERONE_MEDIATED_AUTOPHAGY			0.97	0.93	1.14	0.53		
	MACROAUTOPHAGY	1.30	0.35			1.26	0.4	1.28	0.27
	NEGATIVE_REGULATION_OF_AUTOPHAGY	1.00	0.68			1.38	0.28	1.13	0.45
	NEGATIVE_REGULATION_OF_MACROAUTOPHAGY	1.39	0.29			1.43	0.25	0.9	0.81
	POSITIVE_REGULATION_OF_AUTOPHAGY_OF_MITOCHONDRION	0.88	0.83	0.99	0.91	1.3	0.36	1.26	0.3
	POSITIVE_REGULATION_OF_MACROAUTOPHAGY	1.00	0.68			0.88	0.87	1.05	0.58
	PROCESS_UTILIZING_AUTOPHAGIC_MECHANISM	1.28	0.36	1	0.91	1.12	0.56	1.16	0.41
	REGULATION_OF_AUTOPHAGOSOME_ASSEMBLY	0.92	0.79			1.53	0.19	1.53	0.1
	REGULATION_OF_AUTOPHAGY	1.20	0.44			0.93	0.82	1.07	0.54
	REGULATION_OF_AUTOPHAGY_OF_MITOCHONDRION					1.1	0.58	0.86	0.86
	REGULATION_OF_MACROAUTOPHAGY	1.34	0.32	0.91	0.98	1.11	0.56	1.15	0.43
	SELECTIVE_AUTOPHAGY					0.98	0.74		

Color gradient represents the lowest (red), 50% percentile (white), and highest (blue) FDR q-value within a given treatment.

**Table 3** Facemap linkages of top autophagy-inducing agents across low pH niacinamide treatments

Proposed MOA	Treatment_Dose	Linkage Score				
		Veh 2.5	Veh 5.8	Nam 5.8	Nam 3.8	
<b>mTOR-dependent</b>	activates AMPK/inhibits mTORC1	Metformin_10 µm	0.383	0.28	0.337	0.402
	Ca2+ channel and PKC inhibitor/inhibitor of mTORC1	Nicosamide_0.10 µm	-0.078	0.061	0.132	0.123
	Glucocorticoid/increases PML and PML-Akt dephosphorylation	Prednisolone 21-acetate_20 µm	0.129	0.136	0.124	0.102
		Prednisolone_12.8 µm	0.182	0.185	0.166	0.155
	inhibits mTORC1	Ridaforolimus_0.001 µm	0.113	0.051	0.215	0.275
		Ridaforolimus_0.1 µm	0.101	0.053	0.203	0.261
		Ridaforolimus_1 µm	0.073	0.016	0.173	0.23
	inhibits mTORC1	Temsirolimus_1 µm	0.068	0.009	0.17	0.223
	ATP-competitive mTOR inhibitor	Torin 1_0.001 µm	0.116	0.075	0.237	0.282
	ATP-competitive mTOR inhibitor	Torin 2_0.01 µm	0.076	0.063	0.217	0.285
<b>mTOR-independent</b>	K+ATP channel opener	2,4-Pyrimidinediamine, 6-(1-piperidinyl)-, 3-oxide_10 µm	0.465	0.295	0.388	0.418
	Chemical chaperone	2,4-Pyrimidinediamine, 6-(1-piperidinyl)-, 3-oxide_30 µm	0.379	0.125	0.277	0.292
		Biotin Trehalose Dihydrate_0.01%	0.18	0.082	0.13	0.099
	induces ER stress	Brefeldin A_0.1 µm	-0.185	0.069	-0.063	-0.019
	MIP synthase inhibitor; decreases intracellular inositol phosphatase	Carbamazepine_10 µm	0.1	0.111	0.01	0.039
		Clonidine hydrochloride_10 µm	0.387	0.246	0.328	0.349
		D-(+)-Trehalose dihydrate_10 µm	0.461	0.315	0.324	0.341
	IMPase inhibitor; decreases intracellular inositol phosphatase	Lithi µm chloride_10 µm	0.39	0.307	0.332	0.331
	histone acetyltransferase inhibitor	Spermidine_10 µm	0.143	-0.048	0.09	0.025
	Ca2+ channel blocker and PKC inhibitor/inhibitor of mTORC1	Verapamil hydrochloride_10 µm	0.07	-0.005	0.047	0.032
<b>mTOR-dependent/independent</b>	Ca2+ channel blocker and PKC inhibitor/inhibitor of mTORC1	Amiodarone hydrochloride_1 µm	-0.099	-0.112	-0.11	-0.121
	activates histone deacetylase SIRT-1/ inhibits mTORC1 and S6K	Biotin Resveratrol_1e-04%	0.077	-0.006	0.134	0.126
		HerbEx Resveratrol_0.01%	0.357	0.224	0.258	0.296
	Oxyresveratrol_5 µm	0.085	0.115	0.176	0.154	
	Oxyresveratrol_50 µm	-0.031	-0.093	0.107	0.076	
	Resveratrol_0.01%	-0.062	-0.062	0.148	0.124	
	Resveratrol_10 µm	-0.047	-0.015	0.042	0.029	
	Resveratrol_20 µm	0.257	0.157	0.102	0.146	

Color gradient represents the lowest (blue), 50% percentile (white), and highest (red) linkage score within a given treatment.

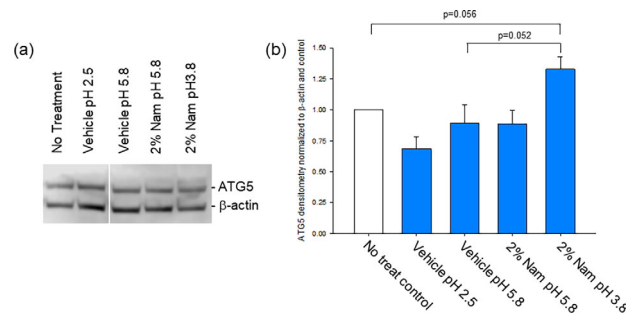


**Figure 4** Nam increases ATG5 protein levels in 3D human epidermal skin equivalent model. (a) MatTek EpiDerm™ cultures were topically treated with skin care formulations that comprised vehicle (pH 2.5), vehicle (pH 5.8), 2% Nam (pH 5.8) or 2% Nam (pH 3.8) for 24 h. Cultures were processed and analysed by immunoblotting using the indicated antibodies.  $\beta$ -Actin served as a control. (b) Densitometric analysis of the signals on the blots ( $n = 3$ ) show a significant increase in ATG5 protein levels by 2% Nam (pH 3.8;  $P = 0.056$ ) compared with non-treated control and vehicle (pH 5.8;  $P = 0.052$ ) cultures. Nam, niacinamide.

normal epidermal differentiation and homeostasis<sup>2,4</sup> as well as in ageing<sup>5</sup> and skin diseases.<sup>3</sup>

Over the past few decades, Nam has become an important molecule in cosmetic and pharmaceutical products for the treatment of acne, skin photoageing attributes, and barrier integrity improvement.<sup>6–8</sup> Nam has been reported to protect cells from oxidative stress, metabolic disruption, and inflammation.<sup>9,10</sup> Relevant to protecting from environmental insults, Nam has also been shown to inhibit acute and chronic damaging effects of UV exposure on skin.<sup>11</sup> Kang *et al.*<sup>27</sup> reported that Nam can increase the *in vitro* lifespan of dermal fibroblasts and it is hypothesized this is via mitophagy, a select form of autophagy, that improves mitochondrial activity.<sup>14</sup> The induction of mitophagy by Nam in fibroblasts is believed to be via maintaining  $NAD^+/NADH$  ratios.<sup>15</sup> To our knowledge, there are no published reports evaluating the role of Nam on autophagy in keratinocytes, a critical cell involved in skin's homeostasis maintenance. We report here that Nam treatment of human epidermal keratinocytes can lead to an induction of an autophagy-related response as measured by autophagosome accumulation and increased gene expression and protein levels of ATG5, a canonical marker of autophagy. Interestingly, the response occurs within 6 h and returns to baseline control levels by 72 h suggesting. It is also worth noting that the response to Nam is relatively low. We believe this is due in part to Nam having a benign impact of cell response under normal culture conditions but can protect cells from oxidative stress.<sup>13</sup> Future work will focus on evaluating Nam effects under conditions of oxidative stress, inflammation and ageing to better understand the kinetics with additional autophagy measurements and markers is merited.

Skin surface pH is acidic compared with internal physiological pH and is estimated to be slightly under pH 5.<sup>28</sup> This lower pH is important in maintaining barrier integrity as well as overall function and turnover,<sup>29</sup> and atopic dermatitis is associated with a higher skin surface pH.<sup>30</sup> It has been measured that with age the skin surface pH increases closer to pH 6.<sup>18</sup> This drift to more

neutral pH is considered to impact skin barrier integrity and overall health.<sup>31</sup> Treatment of skin with lower pH formulations has been attributed to improving barrier integrity as well as various disease conditions such as atopic dermatitis.<sup>32</sup>

Topical formulations containing Nam have historically been practised within a neutral pH range to prevent formation of niacin, a known vasodilator. Previous testing has determined a threshold level of niacin that can trigger a perceptible flushing indication and 2% Nam as final concentration has been previously shown to deliver efficacy of barrier and skin health improvement.<sup>33</sup> Formulation optimization efforts established that lowering the pH to as low as 3.8 would still allow for usage of 2% Nam with minimal niacin formation below the threshold level. Additionally, testing 2% Nam formula at pH 3.8 in a 28-day safety-in-use study found no difference in erythema or dryness as measured in control formulations (data not shown).

Nam at neutral pH had a modest autophagy induction in the 2D models. Partly, this may be due to it being tested under normal growth conditions and may require tested under oxidative stress conditions or with senescence cells. To test what effect lowering the pH range has on Nam mechanistic response, we utilized an epidermal 3D skin model system to compare Nam formulations at varying pH ranges. Bioinformatic analyses identified that 2% Nam formulations at pH 3.8 showed a statistically significant higher induction of the GO term of “positive regulation of autophagy” compared with a 2% Nam formula at pH 5.8 and control formula. This highlights that optimizing the Nam formulation increases its likelihood of elevated efficacy.

In summary, we propose that Nam can induce autophagy in human epidermal keratinocytes under normal growth conditions. Additionally, optimizing formulations of 2% Nam at pH levels as low as 3.8 show a significant induction of autophagy-related gene expression patterns in 3D skin models when compared with neutral pH Nam and pH control formulas. These

findings support the potential for increased clinical efficacy response by low pH Nam formulas on skin ageing appearance metrics. Future work is needed to better understand the mechanistic aspects of autophagy induction as related to mTOR regulation as well as evaluate under stress conditions to more closely mimic *in vivo* conditions.

### Acknowledgement

We thank Laure Moulton for statistical support.

### Authors contributions

Y.M.D., J.C.B., H.A.R., L.V. and T.L. performed cell biology experiments; W.Z. and J.D.S. performed bioinformatics analysis; S.H. and R.K. performed the CMap testing and developed the signature-free pattern matching algorithm, respectively; R.A. performed the microarray analyses. Y.M.D. performed immunoblot analysis; T.L. and B.B.J. performed Cyto-ID<sup>®</sup> analysis; J.E.O., Y.M.D., J.C.B., H.A.R., T.L., W.Z., J.D.S. and T.H. designed and supervised elements of the study; J.E.O. and T.H. supervised the project; J.E.O. wrote the paper with help from all authors.

### References

- Vicencio JM, Galluzzi L, Tajeddine N *et al*. Senescence, apoptosis or autophagy? When a damaged cell must decide its path—a mini-review. *Gerontology* 2008; **54**: 92–99.
- Nagar R. Autophagy: a brief overview in perspective of dermatology. *Indian J Dermatol Venereol Leprol* 2017; **83**: 290–297.
- Guo Y, Zhang X, Wu T, Hu X, Su J, Chen X. Autophagy in skin diseases. *Dermatology* 2019; **235**: 380–389.
- Akinduro O, Sully K, Patel A *et al*. Constitutive autophagy and nucleophagy during epidermal differentiation. *J Invest Dermatol* 2016; **136**: 1460–1470.
- Eckhart L, Tschachler E, Gruber F. Autophagic control of skin aging. *Front Cell Dev Biol*. 2019; **7**: 143.
- Matts PJ, Oblong JE, Bissett DL. A review of the range of effects of niacinamide in human skin. *IFSCC* 2002; **50**: 285–290.
- Wohlrab J, Kreft D. Niacinamide – mechanisms of action and its topical use in dermatology. *Skin Pharmacol Physiol* 2014; **27**: 311–315.
- Surjana D, Damian DL. Niacinamide in dermatology and photoprotection. *Skinmed* 2011; **9**: 360–365.
- Sivapirabu G, Yiasemides E, Halliday GM, Park J, Damian DL. Topical niacinamide modulates cellular energy metabolism and provides broad-spectrum protection against ultraviolet radiation-induced immunosuppression in humans. *Br J Derm* 2009; **161**: 1357–1364.
- Zhang XM, Jing YP, Jia MY, Zhang L. Negative transcription regulation of inflammatory genes by group B3 vitamin niacinamide. *Mol Biol Rep* 2012; **39**: 1036–10371.
- Snaird VA, Damian DL, Halliday GM. Niacinamide for photoprotection and skin cancer chemoprevention: a review of efficacy and safety. *Exp Dermatol* 2019; **28**(Suppl 1): 15–22.
- Chen AC, Damian DL. Niacinamide and the skin. *Australas J Dermatol* 2014; **55**: 169–175.
- Oblong JE. The evolving role of the NAD<sup>+</sup>/nicotinamide metabolome in skin homeostasis, cellular bioenergetics, and aging. *DNA Repair (Amst)* 2014; **23**: 59–63.
- Kang HT, Hwang ES. Nicotinamide enhances mitochondria quality through autophagy activation in human cells. *Aging Cell* 2009; **8**: 426–438.
- Jang SY, Kang HT, Hwang ES. Nicotinamide-induced mitophagy: event mediated by high NAD<sup>+</sup>/NADH ratio and SIRT1 protein activation. *J Biol Chem* 2012; **287**: 19304–19314.
- Lichterfeld-Kottner A, El Genedy M, Lahmann N, Blume-Peytavi U, Büscher A, Kottner J. Maintaining skin integrity in the aged: A systematic review. *Int J Nurs Stud* 2019; **103**: 10350.
- Blaak J, Wohlfart R, Schürer N. Treatment of aged skin with a pH 4 skin care product normalizes increased skin surface pH and improves barrier function: results of a Pilot Study December. *J Cosmet Dermatol Sci Appl* 2010; **1**: 50–58.
- Man MQ, Xin SJ, Song SP *et al*. Variation of skin surface pH, sebum content and stratum corneum hydration with age and gender in a large Chinese population. *Skin Pharmacol Physiol* 2009; **22**: 190–199.
- Sheng J, Sun LB, Zhao SF *et al*. Acidic stress induces protective autophagy in SGC7901 cells. *J Int Med Res* 2018; **46**: 3285–3295.
- Subramanian A, Tamayo P, Mootha VK *et al*. Gene set enrichment analysis: a knowledge-based approach for interpreting genome-wide expression profiles. *Proc Natl Acad Sci USA* 2005; **102**: 15545–15550.
- Mootha VK, Lindgren CM, Eriksson KF *et al*. PGC-1 $\alpha$ -responsive genes involved in oxidative phosphorylation are coordinately downregulated in human diabetes. *Nat Genet* 2003; **34**: 267–273.
- Ashburner M, Ball CA, Blake JA, *et al*. Gene ontology: tool for the unification of biology. *Nat Genet* 2000; **25**: 25–29.
- The Gene Ontology Consortium. The gene ontology resource: 20 years and still going strong. *Nucleic Acids Res* 2019; **47**(D1): D330–D338.
- Lamb J, Crawford ED, Peck D *et al*. The connectivity map: using gene-expression signatures to connect small molecules, genes, and disease. *Science* 2006; **313**: 1929–1935.
- Mills KJ, Robinson MK, Sherrill JD, Schnell DJ, Xu J. Analysis of gene expression profiles of multiple skin diseases identifies a conserved signature of disrupted homeostasis. *Exp Dermatol* 2018; **27**: 1000–1008.
- Fleming A, Noda T, Yoshimori T, Rubinsztein DC. Chemical modulators of autophagy as biological probes and potential therapeutics. *Nat Chem Biol* 2011; **7**: 9–17.
- Kang HT, Lee HI, Hwang ES. Nicotinamide extends replicative lifespan of human cells. *Aging Cell* 2006; **5**: 423–436.
- Lambers H, Piessens S, Bloem A, Pronk H, Finkel P. Natural skin surface pH is on average below 5, which is beneficial for its resident flora. *Int J Cosmet Sci*. 2006; **28**: 359–370.
- Ali SM, Yosipovitch G. Skin pH: from basic science to basic skin care. *Acta Derm Venereol* 2013; **93**: 261–269.
- Surber C, Humbert P, Abels C, Maibach H. The acid mantle: a myth or an essential part of skin health? *Curr Probl Dermatol* 2018; **54**: 1–10.
- Schmid-Wendtner M-H, Korting HC. The pH of the skin surface and its impact on the barrier function. *Skin Pharmacol Physiol* 2006; **19**: 296–302.
- Danby SG, Cork MJ. pH in atopic dermatitis. *Curr Probl Dermatol* 2018; **54**: 95–107.
- Draeos ZD, Ertel K, Berge C. Niacinamide-containing facial moisturizer improves skin barrier and benefits subjects with rosacea. *Cutis* 2005; **76**: 135–141.